COMMISSIONING OF THE RADIABEAM/SLAC DECHIRPER

M. W. Guetg [*1], K. L. F. Bane[1], A. Brachmann[1], A. S. Fisher[1], M. A. Harrison[2], Z. Huang[1], R. Iverson[1], P. Krejcik[1], A. A. Lutman[1], T. J. Maxwell[1], A. Novokhatski[1], M. Ruelas[2], G. Stupakov[1], J. Zemella[1,3], and Z. Zhang[1,4]

[1]SLAC National Accelerator Laboratory, Menlo Park, CA, USA
[2]RadiaBeam Systems, Santa Monica, CA, USA
[3]DESY, Hamburg, Germany
[4]TUB, Beijing, China

Abstract

We present results on the commissioning of the two-module RadiaBeam / SLAC dechirper system at LCLS. This is the first installation and measurement of a corrugated dechirper at high energy (4.4 - 13.3 GeV), short pulses (< 200 fs) and while observing its effect on an operational FEL. Both the transverse and longitudinal wakefields allow more flexible electron beam tailoring. We verify that, for a single module at a given gap, the strength of the longitudinal wake on axis and the dipole near the axis agree well with the theoretical values. Using direct longitudinal phase space mapping and X-ray FEL spectrum measurements we demonstrate the energy chirp control capabilities.

INTRODUCTION

Dechirpers are passive devices intended primarily to control the longitudinal phase space [1–3], specifically the energy chirp. Through enhanced longitudinal wakefields, electron energy chirp control allows the adjustment of the FEL photon pulse bandwidth, potentially increasing the photon brightness.

In addition, transverse wakefields allow for the introduction of beam-tilt (centroid slice shift), which is used to map the beam for longitudinal and transverse reconstruction [4, 5] or selective lasing suppression, allowing ultra-short bunches [6] and two-colors with step-less controllable delay through zero [7]. The installation of two orthogonal dechirpers allows emittance growth compensation [8, 9] and deflection in both transverse planes. The benefit of this passive method lies in its simplicity and its intrinsic beam synchronization.

For flat-top current profiles with short bunches passing through a corrugated structure with flat geometry, the longitudinal wakefield is approximately linear along the bunch, making it ideal for removing residual energy chirp after bunch compression. For this case the mean energy variation is approximated by [10]:

$$\Delta E = -\frac{\pi}{8} \frac{Z_0 c}{g^2} \frac{eQL}{E}, \qquad (1)$$

where Z_0 is the impedance of free space, c the speed of light in vacuum, g the gap between the two corrugated plates,

e the elementary charge, Q the charge of the bunch, L the structure length, and E the bunch energy. The transverse wakefields are approximated by [10]:

$$\langle x' \rangle = \frac{\pi^2}{24} \frac{Z_0 c}{g^3} \frac{eQLl}{E} \sec^2\left(\frac{\pi x}{g}\right) \tan\left(\frac{\pi x}{g}\right), \qquad (2)$$

where l corresponds to the full (rectangular) bunch length. The transverse kick from the dipole wakes growths quadratically from head to tail of the bunch. In the following we show a comparison with respect to the above approximations. Note that the longitudinal wakefields scale with the inverse square of the gap, whereas the transverse wakes scale with the inverse cube. This makes the design of the dechirper a trade-off between module length and required alignment accuracy. Physical parameters of the installed dechirpers are given in the next section.
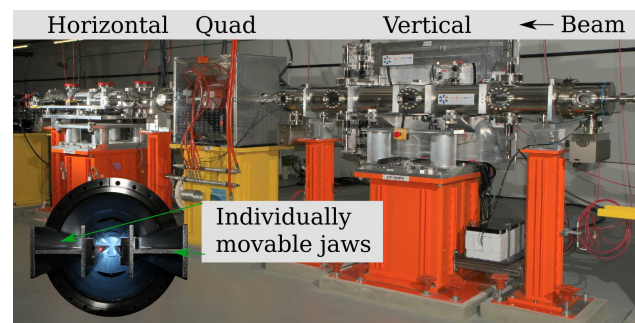
SETUP

Figure 1: The two dechirper modules installed at LCLS. The inset shows the interior of the horizontal module with its corrugation.

Two similar dechirper modules, the first vertical and the second horizontal adjustable gap, (Figure 1) are installed in the LCLS [11] undulator transfer line. The two orthogonal modules are meant to cancel the quadrupole component of the transverse wakefields [8]. Each module consists of two in-vacuum corrugated jaws made of aluminum. Each jaw is individually movable in both pitch and distance from the center, which allows alignment of the individual jaws to reduce dipole kicks from the transverse wakefields. Step motors with encoders move the modules, whereas linear vari-

able differential transformer (LVDT) give an independent position feedback.

A pair of beam-loss fibers was installed along the outside of the vacuum chambers of the two dechirpers. Due to a delay line in the fiber it is possible to detect the loss location by measuring the time it took the light in the fiber to arrive at the sensor. The fibers both supplement already existing radiation monitoring in the accelerator tunnel.

Additional operational parameters of the installed dechirper are listed in Table 1 and given in [12].

Table 1: Physical Parameters of the Radiabeam/SLAC Dechirper Installed at LCLS.

Item	value
Active length / module	2.02 m
Transverse extend	127 ± 0.1 mm
Corrugation period	508 ± 13 µm
Slit gap	254 ± 25 µm
Slit depth	508 ± 25 µm
Gap	0.7 – 25 mm
Pitch	±1 mrad
Motor repeatability	25 µm
LVDT tolerance	50 µm

ALIGNMENT

To ensure maximal FEL performance, the slices of the electron beam need to be well aligned. An orbit offset within the dechirper excites non-canceling linear transverse wakefields, which in turn leads to FEL degradation due to the resulting beam tilt. Equation 2 shows the inverse cubic dependence of the wakefields on the jaw gap, therefore making the alignment crucial especially for small gaps. This section introduces the method used for the individual alignment of both dechirper modules.

The alignment process is based on the transverse wakefields. For the entire process the incoming electron beam is kept steady in orbit, compression and energy. With a constant gap, the mid-position between a pair of opposing jaws is scanned which leads to a deflection of the downstream electron beam. A beam position monitor (BPM) located after a 17 m downstream drift from the dechirper measures the beam's deflected center of mass. Note that the head of the bunch is unaffected by transverse wakefields, but the deflection of the tail shifts the centroid measured by the BPMs. The tail undergoes larger orbit oscillations than the recorded centroid which might lead to losses. A pair of BPM up- and down-stream of the dechirper coupled with an energy measurement allows one to differentiate between incoming orbit errors, both jitter and fixed, and transverse kick originating in the dechirper. Figure 2 compares a deflection scan with theory and shows good agreement. The inverse cubic fit allows one to locates the center of the dechirper with respect to the electron beam, which possibly differs from the metrological center.

Minimization of pitch was achieved by aligning to the two extreme taper (reverse pitch in both jaws). This allowed individual alignment of both the dechirper entrance and exit.
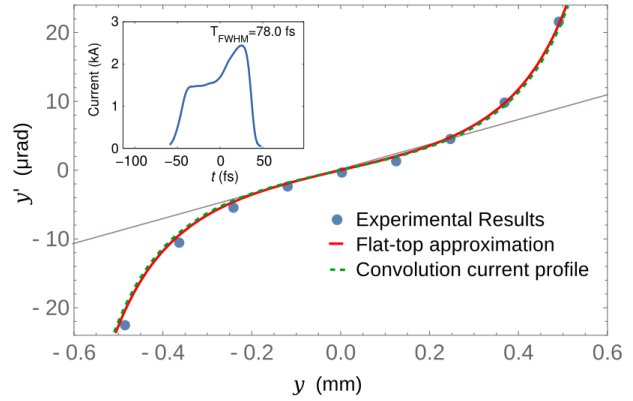

Figure 2: Deflection angle as function of center position in one dechirper module. The theory for the deflection includes a modification of Equation 2 (see [13]). The gap of the simulations was reduced by 200 µm (measured gap was 2 mm) to fit the experimental data.

For the third degree of freedom, symmetric taper of the jaws, absolute readback of dechirper end gap widths was considered sufficient for impact on the beam.

The alignment process could be further improved by scanning both dechirpers at the same time. The time-gain in alignment is however not worth the lost flexibility of aligning each of the four centers individually. Specifically because the beam orbit at this location is very reproducible, making realignments rarely necessary in operations.
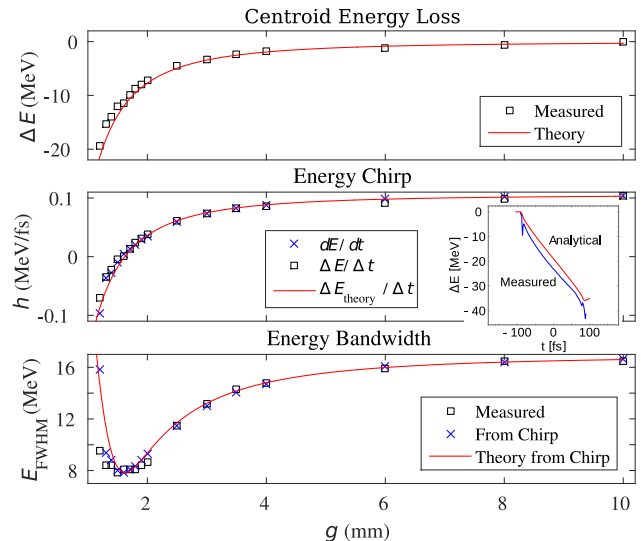

Figure 3: Top: Centroid beam loss measured by a BPM in a dispersive section. Middle: Chirp was measured with a profile monitor at a dispersive section and streaked with a TCAV [14], the inset shows the comparison for one example case ($g = 1.2$ mm). Bottom: Electron bandwidth with a clear minimum, due to horns a 20% scaling was necessary. All scans were taken at 4.425 GeV with flat-top current-profile at 1 kA with 180 pC charge and using both modules.

ELECTRON BANDWIDTH CONTROL

The longitudinal wakefields of the dechirper allow for control of the energy chirp of the electron beam. Figure 3 shows an example scan of the centroid energy loss recorded by dispersive BPM. Since the current-profile was close to flat-top, the energy loss along the beam is to a good approximation linear. Energy chirp was determined by transverse deflecting cavity measurement in the dispersive bend as shown in the middle plot. The analytical result includes a modification to Equation 2 (see [13]). There is very good agreement between theoretical values and measurements.

The cancellation of the incoming residual chirp leads to a reduction of the electron bandwidth (Figure 3, bottom), highlighting the potential to manipulate the energy chirp. Note that the incoming positive energy chirp was deliberately increased by RF phasing. With respect to RF phasing, the dechirper allows us to directly control the energy chirp without changing the beam energy along the linac. This reduces chromaticity and optical mismatch due to relative quadrupole strength errors because of beam energy variation.

PHOTON BANDWIDTH CONTROL

The FEL pulse energy and bandwidth control are the final figure of merits for the dechirper, which are both explored in this section.

Figure 4 shows integrated-photon-spectra recorded for several dechirper gap settings. It shows a reduction of photon central pulse energy with smaller gap-sizes as the electron energy decreases due to the longitudinal wakefields. The initial conditions for this experiment started with minimized electron bandwidth at the dechirper entrance. Therefore closing the dechirper gap increased the photon bandwidth by chirping the electron beam. This clearly demonstrates the photon bandwidth control of the dechirper.
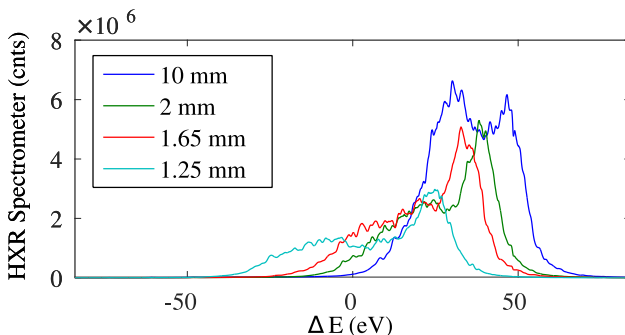

Figure 4: Average photon spectra on 100 single shots from electron beams with same electron beam energy to eliminate wavelength jitter, at various dechirper gap settings. The central photon energy is 8 keV. Here peak-current is 3.6 kA and bunch charge is 180 pC.

Figure 5 shows photon spectra properties corresponding to those of the electrons shown in Figure 3. The photon energy follows exactly the form of the electron energy as expected by simple FEL theory ($\lambda \propto 1/\gamma^2$, where λ is the

fundamental photon wavelength and γ is the Lorentz factor). Similarly, the photon bandwidth follows the electron energy bandwidth, except for very small gaps. The lack of increase of photon bandwidth is believed to originate from lasing suppression at the tail of the electron bunch due to transverse wakefields. Those can either be dipole kicks due to beam-tilt going into the dechirper (centroid position was aligned) or higher order contributions changing the slice-spot-size and therefore the slice-match.
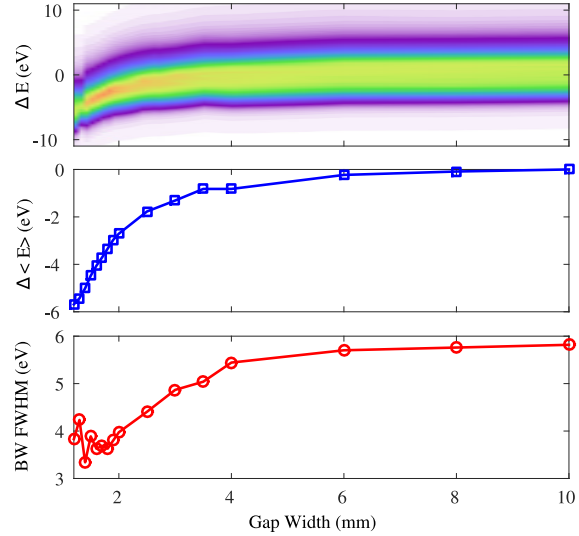

Figure 5: Top: Energy binned averaged (100) spectra as function of the gap width. Middle: Photon mean energy. Bottom: Photon bandwidth. Electron bunch energy 4.425 GeV (dechirper out) with 180 pC bunch charge and 1 kA peak current.

CONCLUSION

This report describes the successful commissioning of the two RadiaBeam / LCLS dechirper modules installed in LCLS. It emphasizes specifically the crucial transverse alignment using transverse wakefields. The transverse deflection was found to be very well predicted by theory.

This work also demonstrates the dechirper's longitudinal phase space tuning capabilities. Both electron energy decrease and chirp generation show good agreement with theory. We furthermore demonstrate the first photon bandwidth control using a dechirper on an active FEL machine by both increasing and decreasing the photon bandwidth.

Further advanced schemes, mainly using the transverse wakefields for selective lasing suppression, are currently under investigation.

ACKNOWLEDGMENT

REFERENCES

[1] K.L.F. Bane and G. Stupakov. Corrugated pipe as a beam dechirper. *Nuclear Instruments and Methods in Physics Research Section A: Accelerators, Spectrometers, Detectors and Associated Equipment*, 690:106 – 110, 2012.

[2] A. Novokhatski. Wakefield potentials of corrugated structures. *Phys. Rev. ST Accel. Beams*, 18:104402, Oct 2015.

[3] G. Stupakov and K. L. F. Bane. Surface impedance formalism for a metallic beam pipe with small corrugations. *Phys. Rev. ST Accel. Beams*, 15:124401, Dec 2012.

[4] S. Bettoni, P. Craievich, A. A. Lutman, and M. Pedrozzi. Temporal profile measurements of relativistic electron bunch based on wakefield generation. *Phys. Rev. Accel. Beams*, 19:021304, Feb 2016.

[5] Alexander Novokhatski, Axel Brachmann, Massimo Dal Forno, Valery Dolgashev, Alan Stephen Fisher, Marc Walter Guetg, Zhirong Huang, Richard Iverson, Patrick Krejcik, Alberto Andrea Lutman, Timothy John Maxwell, and Johann Zemella. RadiaBeam/SLAC Dechirper as a Passive Deflector. Number MOPOW046, Busan, 2016.

[6] Eduard Prat, Florian Löhl, and Sven Reiche. Efficient generation of short and high-power x-ray free-electron-laser pulses based on superradiance with a transversely tilted beam. *Phys. Rev. ST Accel. Beams*, 18:100701, Oct 2015.

[7] Alberto Luttman. Personal communication.

[8] Zhen Zhang, Karl Bane, Yuantao Ding, Zhirong Huang, Richard Iverson, Timothy Maxwell, Gennady Stupakov, and Lanfa Wang. Electron beam energy chirp control with a rectangular corrugated structure at the linac coherent light source. *Phys. Rev. ST Accel. Beams*, 18:010702, Jan 2015.

[9] Feichao Fu, Rui Wang, Pengfei Zhu, Lingrong Zhao, Tao Jiang, Chao Lu, Shengguang Liu, Libin Shi, Lixin Yan, Haixiao Deng, Chao Feng, Qiang Gu, Dazhang Huang, Bo Liu, Dong Wang, Xingtao Wang, Meng Zhang, Zhentang Zhao, Gennady Stupakov, Dao Xiang, and Jie Zhang. Demonstration of nonlinear-energy-spread compensation in relativistic electron bunches with corrugated structures. *Phys. Rev. Lett.*, 114:114801, Mar 2015.

[10] K. Bane and G. Stupakov. Dechirper wakefields for short bunches. *Nuclear Instruments and Methods in Physics Research Section A: Accelerators, Spectrometers, Detectors and Associated Equipment*, 820:156 – 163, 2016.

[11] P. Emma, R. Akre, J. Arthur, R. Bionta, C. Bostedt, J. Bozek, A. Brachmann, P. Bucksbaum, R. Coffee, F.-J. Decker, Y. Ding, D. Dowell, S. Edstrom, A. Fisher, J. Frisch, S. Gilevich, J. Hastings, G. Hays, Ph. Hering, Z. Huang, R. Iverson, H. Loos, M. Messerschmidt, A. Miahnahri, S. Moeller, H.-D. Nuhn, G. Pile, D. Ratner, J. Rzepiela, D. Schultz, T. Smith, P. Stefan, H. Tompkins, J. Turner, J. Welch, W. White, J. Wu, G. Yocky, and J. Galayda. First lasing and operation of an ångstrom-wavelength free-electron laser. *Nature Photonics*, 4(9):641–647, aug 2010.

[12] M.A. Harrison, Marcos Ruelas, Jacob McNevin, Pedro Frigola, and Alex Murokh. Implementation of a Corrugated-Plate Dechirping System for Gev Electron Beam at LCLS. Number MOPOW049, Busan, KOR, 2016.

[13] K. Bane, G. Stupakov, and I. Zagorodnov. Analytical formulas for short bunch wakes in a flat dechirper. *SLAC-PUB-16497*, 2016.

[14] C. Behrens, F.-J. Decker, Y. Ding, V. A. Dolgashev, J. Frisch, Z. Huang, P. Krejcik, H. Loos, A. Lutman, T. J. Maxwell, J. Turner, J. Wang, M.-H. Wang, J. Welch, and J. Wu. Few-femtosecond time-resolved measurements of x-ray free-electron lasers. *Nature Communications*, 5, apr 2014.

02 Photon Sources and Electron Accelerators

A06 Free Electron Lasers